INTERNATIONAL JOURNAL OF CIRCUITS, SYSTEMS AND SIGNAL PROCESSING
DOI: 10.46300/9106.2020.14.46 Volume 14, 2020

An Image Fusion Algorithm based on Modified Contourlet Transform

Pai Zhang
College of Intelligence and Information Engineering
Tangshan College, China

Received: May 10, 2020. Revised: June 17, 2020. Accepted: July 3, 2020. Published: July 20, 2020.

Abstract— Multi-focus image fusion has established itself as a useful tool for reducing the amount of raw data and it aims at overcoming imaging cameras' finite depth of ield by combining information from multiple images with he same scene. Most of existing fusion algorithms use the method of multi-scale decompositions (MSD) to fuse the ource images. MSD-based fusion algorithms provide much better performance than the conventional fusion methods .In the image fusion algorithm based on multi-scale decomposition, how to make full use of the characteristics of coefficients to fuse images is a key problem.This paper proposed a modified contourlet ransform(MCT) based on wavelets and nonsubsampled directional filter banks(NSDFB). The image is decomposed in wavelet domain,and each highpass subband of wavelets is further decomposed into multiple directional subbands by using NSDFB. The MCT has the important features of directionality and translation invariance. Furthermore, the MCT and a novel region energy strategy are exploited to perform image fusion algorithm. simulation results shows hat the proposed method can the fusion results visually and also improve in objective evaluating parameters.

Keywords—WBCT, NSDFB, image fusion, region energy feature.

I. INTRODUCTION

Multi-scale and multi-direction decomposition are important features of image transformation[1-3]. In recent years, scholars have proposed many new methods for multi-scale geometric analysis of images. Do and Vetterli introduced the contourlet transform [4,5], which can effectively epresent an image containing the contour of a curve. Elsami et al. further proposed a new image transformation without edundancy--wavelet Contourlet transform (WBCT)[6]. Compared with the original Contourlet transform, this transform has number of directions, which can be more effective in the representation of images and successfully applied to the wavelet image coding algorithm.WBCT (and the other based on contourlet transform)has gibbs effect , in order to solve this problem, this paper proposes a new image transform based on wavelets and the non-sampling direction ilter bank, referred as modified contourlet transform MCT).The wavelet transform is applied to perform multi-scale decomposition of the image. Then in the high frequency subband, the nonsubsampled directional filter banks (NSDFB) [7] are exploited to perform multi-direction decomposition of the image, which can represent the image more sparsely[8].

However, almost all fusion algorithms presented so far are based on relatively basic processing techniques and do not consider subjectively relevant information from higher scales of region energy. It is shown this does not always satisfy the complex demands and a more subjectively meaningful method is required.

This paper presents some initial results of a fusion framework based on the idea that subjectively relevant fusion could be achieved if information at higher levels of abstraction such as image energy in diffierent levels are used to guide the basic signal-level fusion process. The MCT has been performed in image fusion application and employed an improved region energy features as the fused strategy. The simulations demonstrate that the proposed MCT based image fusion algorithm achieves better performance compared with other previous fusion algorithms[9,10] . Such a multi-level method is able to eliminate undesirable effects such as fusion artefacts and loss of visual information, generally improve the quality of the fused image and overall reliability of the fusion process.

II. THE MCT CONSTUCTION

Here the image transform based on MCT is developed by using wavelets basis as the multiscale subband decomposition. In wavelet domain, the NSDFB is exploited to the highpass subbands [11]to further perform multidirection decomposition, and the process is shown in Fig.1.

consider that the three highpass bands in wavelet domain are corresponding to the LH, HL, and HH bands[12]. NSDFB is performed at the same number of directions to each band in a given scale (j).The maximum number of directions is set to $N_D = 2^L$ on the finest scale J in wavelet domain , it is proceed through the coarser scales ($j < J$) . In this way, it can achieve the anisotropy scaling law and also overcome pseudo-Gibbs phenomena around singularities.

Taking the HH subband as an example, Fig.1 shows a schematic plot of the MCT using 3 wavelet scales and $L = 3$ directional scales. However, due to the lack of adaptability of the wavelet filter in the directional decomposition, the fully decomposed NSDFB is used at each band.Fig.2 is the spectrum diagram of MCT at the third wavelet scale, in which there are 8 directional decomposition.

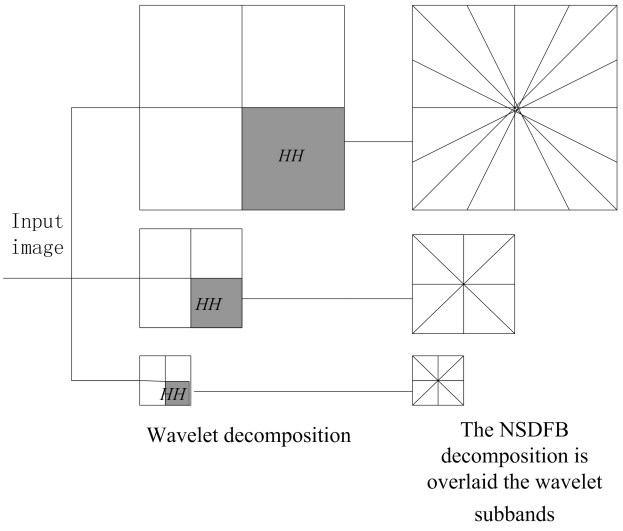

Fig.1 A schematic plot of the MCT using 3 wavelet scales and the directional decomposition is overlaid the wavelet subbands.

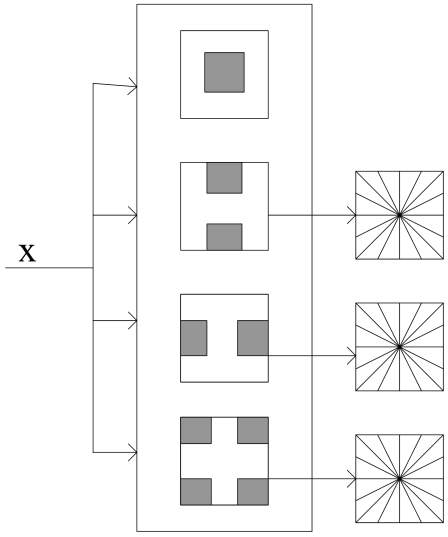

Fig. 2 The schematic diagram of the MCT

III. IMAGE FUSION ALGORITHM BASED ON MCT

In this paper, the proposed MCT image fusion algorithm is characterized by the application of pixel and region information to the fusion process[13,14].In the MCT domain, the related subbands are partitioned into subblocks and the energy value of each subblock is calculated.By using the fusion strategy, and the sparse coefficient is fused by the fusion method based on pixel energy.This method can capture and save the anisotropic edge information and detail information of the image[15].In addition , MCT is almost shift-invariant as the MSD method , when a local energy operator is provided as the fusion strategy to deal with the coefficient sub-blocks , it will not yield blocks artifical phenomenon and capture the region detail information accurately.

Step 1:consider two source images A and B to be fused. Discomposed source images via MCT and illustrate one of them, the mapping is considered to be of the form:

$$x^0 \to \left\{ y^1, y^2, \cdots y^K, x^K \right\} \tag{1}$$

where, y^k is the detail image at scale k and x^K is the appriximation at the coarsest scale K. Then y^k, $k = 1,2 \cdots K$ is further separated into subbands according to its direction, namely, $y^k = \{y_1^k, y_2^k, \cdots, y_D^k\}$ ($y_d^k, d \in [1, D] k \in [1, K]$) representing D directions. Here, the same the number of bidirectional subbands are set on all high-frequency scales , in order to prepare a combination of region-based energy values on the same cross-scale subbands, which can capture and save the anisotropic edge information and detail information of images.

Step2: (1)Divides y_d^k into subregions which can be represented as $\left\{ y_d^k(1), y_d^k(2), \cdots, y_d^k(P) \right\}$, P is the num of subregions. And the energy is caculate values of $y_d^k(p)$, $p \in [1, P]$ .consider that one coefficient is represented by $y_d^k(p)\ (i, j)$ in pth subregion.The energy value can be calculated by following formula:

$$E_d^k(p) = \sum_{i \in I, j \in J} y_d^k(p)(i, j)^2 \tag{2}$$

I, J are the sizes of subregions.

(2)In all high-frequency scales, making a combination energy values of the subregions which are located in the same position of the same directional subbands, the algorithm is caculated as follows:

$$Sum\_E_d(p) = \sum_{k \in K} E_d^k(p) \tag{3}$$

Step3: (1)consider $Sum\_E^{(1)}{}_d(p)$ and $Sum\_E^{(2)}{}_d(p)$ are from image A and B respectively. A map matrix can be generated by comparing two energy values:

$$map(p) = \begin{cases} 1 & Sum\_E^{(1)}{}_d(p) \geq Sum\_E^{(2)}{}_d(p) \\ 0 & Sum\_E^{(1)}{}_d(p) < Sum\_E^{(2)}{}_d(p) \end{cases} \tag{4}$$

The number of subregions determines the size of the map matrix.Each element of matirx is a matching measurement parameter, indicating which corresponding subregion of the source image should be adopted by the fused image.

(2)Because of detail complexity of source image ,in some subregions ,it may have some miscarriage of justice by only using the region-based energy fuse strategy .To solve the problem, two effective rules are projected for the map matrix, stated as follows:

Firstly, a 3×3 window filter of the form $W = \begin{bmatrix} 1 & 1 & 1 \\ 1 & 1 & 1 \\ 1 & 1 & 1 \end{bmatrix}$ is constracted and applied to filter the map matrix. if corresponding elements values of certain subregions in the matrix are not same as all the neighbors' around them. The situation is regarded as a miscarriage of justice. Then this

approach can slove the problem. the concrete rule are stated in Equation(5) .

$$map(p)=\begin{cases}1 & if \sum\limits_{\substack{i\in[-1,1]\\ j\in[-1,1]}} map(p+i,p+j)\geq 6\\ 0 & else\end{cases} \tag{5}$$

When both the contours and the texture are present, there is sometimes a cross between the clear and fuzzy areas of the source image. a rule is used to pick the corresponding elements of these subregions in the map matrix.

$$map(p)=\begin{cases}1 & if \sum\limits_{\substack{i\in[-1,1]\\ j\in[-1,1]}} map(p+i,p+j)\geq 7\\ 0 & if \sum\limits_{\substack{i\in[-1,1]\\ j\in[-1,1]}} map(p+i,p+j)\leq 3\\ 3 & if\ 3<\sum\limits_{\substack{i\in[-1,1]\\ j\in[-1,1]}} map(p+i,p+j)<7\end{cases} \tag{6}$$

(3) The method of PEM is stated as follows:

when it encounters $map(p)=3$,that means the corresponding subregion is located in the crisscross position between the clear region and the fuzzy region of the source image.These subregions are composed of clear partial coefficients and fuzzy partial coefficients, so it is difficult to classify them as a whole.In order to better preserve the details of these subregions, the rule of pixel value measurement maximum (PEM) is directly adopted to make the fusion image more accurate by comparing the discernable coefficients of each coefficient value of the two source images with the clear or fuzzy parts.

(4) The method of PEM is stated as follows:

$$E\_pixel_d^k(p)(i,j)=\sum_{\substack{p\in[-1,1]\\ q\in[-1,1]}}\left[y_d^k(p)(i+p,j+q)^2\right] \tag{7}$$

(i,j) is the coefficient direction of subregions.

(5) Choose a approprate measure maximum-based rule in term of the elements of map matrix.The rule is chosen by :

$$Fusion\_rule=\begin{cases}REM & if\ map(p)=0 or\ 1\\ PEM & if\ map(p)=3\end{cases} \tag{8}$$

consider $y^{(1)k}_d(p)$ and $y^{(2)k}_d(p)$ are from source image A and B respectively and the REM is performed as follows:

$$y_d^k(p)=\begin{cases}y^{(1)k}_d(p) & if\ map(p)=1\\ y^{(2)k}_d(p) & if\ map(p)=0\end{cases} \tag{9}$$

consider $E\_pixel^{(1)k}_d(p)(i,j)$ and $E\_pixel^{(2)k}_d(p)(i,j)$ are the coefficient energy values of source image subregions respectively. PEM is performed as follows:

$$y_d^k(p)(i,j)=\begin{cases}y^{(1)k}_d(p)(i,j) & if\ E\_pixel^{(1)k}_d(p)(i,j)\\ & \geq E\_pixel^{(2)k}_d(p)(i,j)\\ y^{(2)k}_d(p)(i,j) & if\ E\_pixel^{(1)k}_d(p)(i,j)\\ & <E\_pixel^{(2)k}_d(p)(i,j)\end{cases} \tag{10}$$

Step4: By performing the same process of highpass subbands, the lowpass subbands are fused in MCT domain and obtained coefficient matrix $x(K)$ .Then exploiting the selected-out $x(K)$ and y_d^k ,the fused image is reconstructed via inverse MCT.

IV. EXPERIMENTAL RESULTS AND ANALYSIS

The objective evaluation of the fusion image should accord with the subjective evaluation, that is to say, the statistical parameter characteristics of the image should accord with the visual perception of human eyes. For the evaluation of multi-sensor image fusion effect, the richness of image information and the maintenance of spatial edge details of source image should be considered. The evaluation indexes adopted in this paper are:

(1) Mutual information[16]: an important concept in infor mation theory, which can be used as a measure of the correlati on between two variables. Therefore, mutual information can be used to measure the correlation between the fusion image a nd the source image to evaluate the fusion effect. The larger th e value, the more information the fusion image obtains from th e source image, and the better the fusion effect. The mutual inf ormation between the fusion image and the source image A an d B is expressed as follows:

$$I_{FA}=\sum_{k=0}^{L-1}\sum_{i=0}^{L-1}P_{FA}(k,i)\log 2\frac{P_{FA}(k,i)}{P_F(k)P_A(i)} \tag{11}$$

$$I_{FB}=\sum_{k=0}^{L-1}\sum_{j=0}^{L-1}P_{FB}(k,j)\log 2\frac{P_{FB}(k,j)}{P_F(k)P_B(j)} \tag{12}$$

Where, P_A, P_B and P_F are the probability density of image A, B and F, $P_{FA}(k,i)$ and $P_{FB}(k,i)$ and is the joint probability density of fusion image and source image respectively.In this paper, the information sum of the fusion image including the source image is taken as the total mutual information, and then divided by the sum of the information entropy of the source image, which is normalized to:

$$MI=\frac{I_{FA}+I_{FB}}{H_A+H_B} \tag{13}$$

(2)EFQI (edge-dependent fusion quality index) [17]. EFQI is a new objective index for evaluating the quality of fusion images proposed in recent years, which can reflect the edge retention of fusion images and the strength of ringing effect around the edges.

It is defined as: $Q_E(A,B,F)=Q_W(A,B,F)^{1-\alpha}\cdot Q_W(A',B',F')^{\alpha}$

Where Q_E is EFQI, Q_W is the weighted fusion evaluation

index. , A' , B' and F' are the edge images of source image A,B and fusion image respectively. Parameter $\alpha \in [0,1]$ reflects the importance of the edge image in the original image.

To evaluate the performance of the proposed fusion algorithm, it is compared with Infrared and Visible image fusion methods and applications(IaV) [18], Remote Sensing Image Fusion With Deep Convolutional Neural Network(DCNN)[19] and Remote Sensing Image Fusion With Deep Convolutional Neural Network (CAB)[20] image fusion algorithms. Objective criteria on MI and $Q^{AB/F}$ are listed in Table I .

Table I The comparison of objective criteria of four fused methods

Images	Fused method				
	Criteria	IaV	DCNN	CAB	Proposed
ClockA/B	MI	6.6302	7.0805	7.4093	9.3788
	$Q^{AB/F}$	0.6820	0.7184	0.7272	0.8438
LenaA/B	MI	5.5935	6.1810	6.3521	8.4983
	$Q^{AB/F}$	0.5642	0.6008	0.6372	0.8024
HoedA/B	MI	6.9539	7.0111	7.4138	9.5588
	$Q^{AB/F}$	0.6713	0.6858	0.7787	0.9707
CT&MIR	MI	3.0299	4.0208	4.2104	6.3626
	$Q^{AB/F}$	0.6147	0.6315	0.6784	0.9353

Table I shows that MI and $Q^{AB/F}$ values of the proposed algorithm are the largest. It is shown that proposed method is the best fusion algorithm with the greatest MI and $Q^{AB/F}$ in multifocus image fusion. It proves that the fused image of the proposed algorithm is strongly correlated with the source images and more image features are preserved in the fusion process. When all is said and done, the proposed algorithm outperforms other algorithms, no matter in visual observation and objective evaluation criterion.

Three multi-focus images(256×256 in size and 256 scales in gray)is selected for testing. One of the fusion results using source image clocks are shown in Fig. 3.

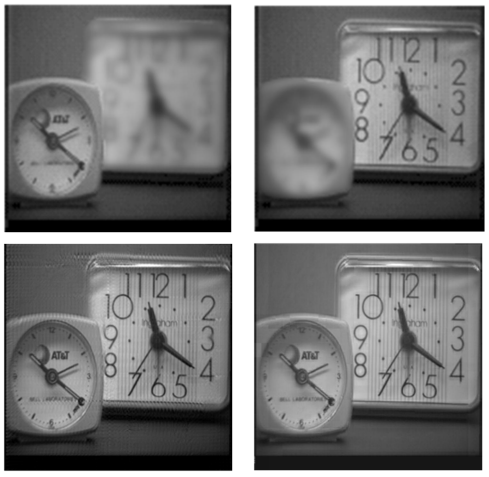

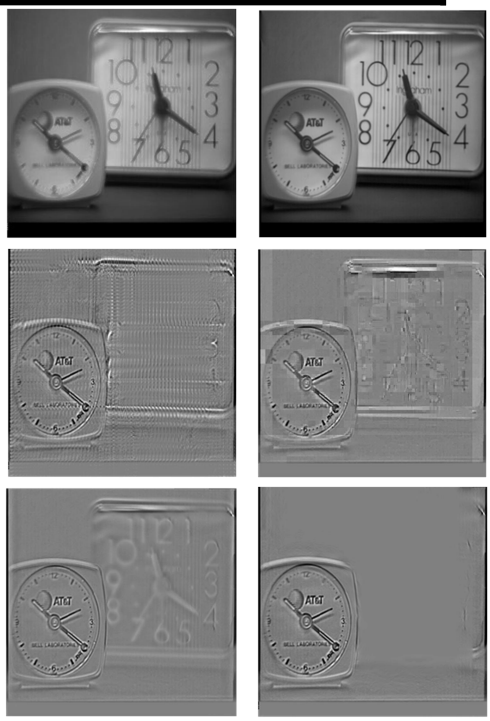

Fig. 3 Clock image fusion results
From top to bottom: clockA(focus on left)clockB(focus on right) Fused images by using IaV, DCNN, CABand the proposed image fusion methods respectively; Difference images among clockB image and the listed fused images.

Fig. 3 shows that the fused image of IaV method is not satisfactory in visual observation, the reason is that difference between source images are slight and transitional regions often exist because of many vague pixels. Only using regional features as fusion strategy, the coefficients cannot be selected accurately. And DCNN methods is also not excellent visually

for its MSD schemes is not shift-invariant. Though CAB has better performance than other two methods , because of lacking a better representation of the contours and textures of NSCT , so its fused image is not possess of advantage than the proposed fused result. Experiments show that the proposed method outperforms other fused method visually.

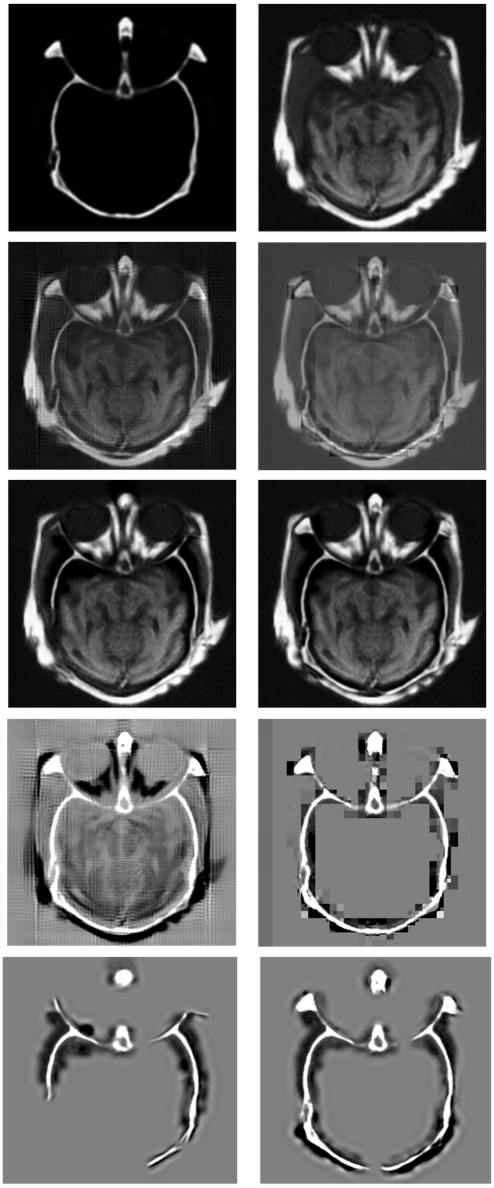

Fig. 4 Medical image fusion results
From top to bottom :CT image; MRI image; Fused medical images by using IaV, DCNN, CABand the proposed image fusion methods respectively; Difference images among CT image and the listed fused images.

The proposed method is also applied to medical image fusion. The CT image shows the structures of bone, and MRI image shows areas of soft tissue. However, in clinical applications, the position of both bone and tissue should be provided to the doctors to determine pathology and aid in diagnosis. So it is need to do medical image fusion and the fusion results are shown in Fig. 4.

From Fig. 4 , it is obviously that fused image of IaV fusion method contrains artificial texture ; The fused image of DCNN method yields blocks aliasing phenomenon. and the fused image of CAB method is inaccurate for losing some details of source CT image. Obviously, the proposed method is excellent to others.

V. Conclusion

In this paper, a new MCT based on wavelets and NSDFB, is proposed and applied to the image fusion field. The simulation results show that the proposed MCT method with the novel region energy strategy, achieves the largest mutual information and $Q^{AB/F}$ values and high quality fused image there by resulting in better performance than existing image fusion methods.

This paper may have useful applications in Medical imaging, and in multisensor image fusion field. However, the region energy strategy fusion rules used here are only some of the numerous region energy strategy fusion tools available and further research should involve a thorough investigation of this particular strategy .

References

[1] Chen, Xiaoying, 'Texture feature extraction method for ground nephogram based on contourlet and the power spectrum analysis algorithm," Cmc-computers materials & continua, vol. 61, no. 2, pp. 861-875, Apr. 2019.

[2] Nayak;Deepak Ranjan, "Automated detection of brain abnormalities using multi-directional features and randomized learning: a comparative study,"Handbook of research on advancements of artificial intelligence in healthcare engineering 2020, pp. 20-41.

[3] KAPURIYA, B. R., PRADHAN, Debasish; SHARMA, Reena. "Detection and restoration of multi-directional motion blurred objects," Signal, image and video processing vol. 13, no. 5, pp. 861-875, 2019.

[4] Do M N., "Directional multiresolution image representations,"Swiss Federal Institute of Technology 2001.

[5] M N Do.,M Vetterli,"The contourlet transform:an efficient directional multiresolution image representation ,"IEEE transactions on image processing,vol.14, no.12, pp. 861-875, 2019.

[6] Subhedar, Mansi S.;and Vijay H. Mankar. "Image steganography using redundant discrete wavelet transform and qr factorization," Computers & electrical engineering 2016, pp.406–422.

[7] Sandstrem. "Topological nearest-neighbor filtering for sampling-based planners," 2018 IEEE international conference on robotics and automation (ICRA) 2018, pp.3053–3060.

[8] Shrestha; Anup; Inanc Senocak. "Multi-level domain-decomposition strategy for solving the eikonal equation with the fast-sweeping method," IEEE Transactions on Parallel and Distributed Systems 2018,vol. 29, no.10, pp. 461-475, 2018.

[9] Pomrehn, Ch. Application of pansharpening algorithms for the fusion of raman and conventional brightfield microscopy images,"2018 9th workshop on hyperspectral

image and signal processing: evolution in remote sensing (WHISPERS) 2018, pp. 1–5.
[10] Shibata;Takashi. "Unified image fusion framework with learning-based application-adaptive importance measure," IEEE transactions on computational imaging vol. 5, no. 1, pp. 82–96, 2019.
[11] Dolganova, Irina N. "Nanoparticle-enabled experimentally trained wavelet-domain denoising method for optical coherence tomography,"Journal of biomedical optics, vol. 61, no. 2, pp. 861-875, 2019.
[12] Mehta; Rajesh. "Robust image watermarking scheme in lifting wavelet domain using ga-lsvr hybridization,"International journal of machine learning and cybernetics .vol. 9, no. 1,pp.145–161,2018.
[13] Koichi; Matsumura. "Image capturing apparatus capable of generating and adding pixel region information to image data, "Method of controlling the same, and image sensor. 2018.
[14] Acharya; U.Rajendra. "Automated characterization of coronary artery disease, myocardial infarction, and congestive heart failure using contourlet and shearlet transforms of electrocardiogram signal," Knowledge vol. 132, pp. 156–166, 2017.
[15] Fazlali;H. R. "Adaptive blind image watermarking using edge pixel concentration," Multimedia tools and applications vol. 76, no. 2 , pp.3105–3120,2017.
[16] Rodriguez. Fernandez; Javier. "Frequency-domain compressive channel estimation for frequency-selective hybrid millimeter wave MIMO systems," IEEE transactions on wireless communications,vol.17, no. 5,pp.2946–2960,2018 .
[17] Qu Xiao-Bo; Yan Jing-Wen;Zhu Zi-Qian; Chen Ben-Gang. "Multi-focus image fusion algorithm based on regional firingcharacteristic of pulse coupled neural networks,". In Proceedings of International Conference on Bio-Inspired Computing Theories and Applications 2007, 563-565.
[18] Ma J, Ma Y, Li C, et al. "Infrared and visible image fusion methods and applications: A survey," Information Fusion, 2018: pp. 153-178.
[19] Shao Z, Cai J. "Remote Sensing Image Fusion With Deep Convolutional Neural Network," IEEE Journal of Selected Topics in Applied Earth Observations and Remote Sensing, vol. 11, no. 5, pp. 1656-1669, 2018.
[20] Farid M S, Mahmood A, Almaadeed S, et al. "Multi-focus image fusion using Content Adaptive Blurring," Information Fusion, 2018, pp.96-112.

Pai Zhang (M'02–SM'06–F'09) received the B.S. and the M.S.degree in School of information engineering from Yanshan University, China, in 2006 and 2009 respectively, Ph.D. degrees in School of electrical engineering from the Yanshan University, Qinhuangdao, China, in 2013.From 2013 to now, she worked at College of Intelligence and Information Engineering Tangshan College, China,. Her current research interest is in the area of multiscale signal processing and applications in image analysis.